AIAA JOURNAL
Vol. 40, No. 8, August 2002

Airfoil-Boundary Layer Subjected to a Two-Dimensional Asymmetrical Turbulent Wake

Vladimir I. Kornilov*
Russian Academy of Sciences, Novosibirsk, 630090, Russia
and
Guy Pailhas† and Bertrand Aupoix‡
Office National d'Etudes et de Recherches Aerospatiales, 31055 Toulouse Cedex 4, France

The results of an experimental study of interaction between an incompressible two-dimensional asymmetrical turbulent wake produced by a symmetrical airfoil at incidence and a boundary layer formed on a similar airfoil immediately downstream are discussed. Extensive measurements of time-averaged quantities of the flow and turbulence characteristics in the interaction region are performed. Particular attention is paid to analysis of the flow structure with the downstream airfoil position being changed across the wake. In particular, a significant reduction in the level of turbulent velocity fluctuations has been found in the boundary layer if the airfoil is located in the wake periphery. A similar effect also has been registered in the outer flow region (outside the boundary layer) for the case when the wing is located in the central part of the wake. Although the interaction process has rather a complicated character, the distribution of the normalized mean velocity defect in the outer region of the interacting flow can be roughly described in the frame of well-known correlations valid for a wake flow immediately downstream of a transverse-positioned circular cylinder. A detailed analysis of the interacting flow components (i.e., isolated turbulent wake and boundary layer) is presented, and a possibility of their description in self-similar variables is shown.

Nomenclature

AR	=	wing aspect ratio
b	=	wake width
C_f	=	local skin-friction coefficient
C_p	=	static-pressure coefficient, $(P - P_\infty)/q$
c	=	chord length
H	=	boundary-layer shape factor, $H = \delta^*/\delta^{**}$
l	=	effective wing span
P	=	static pressure
q	=	dynamic pressure, $\rho u^2/2$
Re	=	Reynolds number
t	=	airfoil thickness
u	=	streamwise velocity component
u'	=	streamwise velocity fluctuation
x	=	coordinate measured from leading edge or trailing edge of the wing parallel to freestream direction
y	=	coordinate normal to x–z plane, distance from wall
z	=	spanwise coordinate
α	=	angle of attack
δ^*	=	displacement thickness
δ^{**}	=	momentum thickness

Subscripts

a	=	airfoil
c	=	based on airfoil chord
e	=	conditions at the boundary-layer edge or in outer wake region
is	=	isolated
max	=	maximum value
min	=	minimum value
s	=	section
W, L	=	windward, leeward
w	=	conditions at the airfoil surface
1	=	based on length of 1 m
∞	=	freestream conditions

Superscript

(-)	=	time-averaged value

Received 10 December 1998; revision received 20 January 1999; accepted for publication 31 January 1999.

*Assistant Professor and Leading Scientist, Department of Experimental Aerodynamics, Institute of Theoretical and Applied Mechanics, Siberian Branch.

†Research Scientist, Department of Models for Aerodynamics and Energetics.

‡Research Director and Head of Research Unit, Department of Models for Aerodynamics and Energetics.

I. Introduction

THE problem of interaction between a turbulent wake produced by a flow around a body and a boundary layer formed on a surface immediately downstream (especially a curved surface) is an important but poorly studied problem of viscous fluid dynamics. This problem can be part of a more complicated problem because the turbulent wake can produce a number of adverse phenomena on a downstream surface, up to a buffetlike phenomenon.[1] From the practical point of view, such a wake can lead to a loss of lifting properties of the surface downstream and considerable spanwise loads, and thus present a significant danger for flying vehicles that are in the wake influence region. The most adverse phenomena are known to occur when the wake contains intense tip vortices. However, the rate of climb of an aircraft can decrease even if there are no tip vortices because the central part of the wake has a downward velocity vector component.

Modeling of interacting flows that develop under the conditions of an increased turbulence of the wake, and its significant asymmetry, involves certain difficulties caused by several reasons. The main reason is that the process under study is strongly nonlinear, which is primarily caused by a nonequilibrium (according to Clauser[2]) character of initial flow produced by the upstream surface. Initially, such a flow is usually formed under the conditions of a streamwise pressure gradient, which, as is shown by experiments of Cousteix and Pailhas[3] and Cousteix et al.,[4] decreases intensely along the wake itself. This flow relaxes gradually to a state of full hydrodynamic

equilibrium that, depending on specific conditions, is achieved at a distance from several tens to several hundreds and even thousands of reference lengths of the body. For these reasons the character of interaction of the system nonequilibrium wake/boundary layer becomes much more complicated.

Another aspect of the problem has a direct relationship to the development of effective numerical methods and generation of a suitable physical model of the flow. This is a necessity of improving the calculation procedures for the flow around a curved surface with regard for the turbulent wake effect. Despite a long time history, this problem has no proper theoretical justification. Although the Navier–Stokes equations that describe such a flow are known in principle, their solution faces certain difficulties, even taking into account the latest achievements in the field of computational aerohydrodynamics. In this case an explicit approximation of all terms of the transport equations for the Reynolds stresses is needed to solve the closure problem. This, in turn, complicates significantly the turbulence model itself, which is based to a large extent on experimental data. Thus, the development and improvement of the flow modeling process and the development of effective methods for calculating this class of flows require accurate information on the structure, transport mechanisms, and regularities of flow evolution in a wide range of varied conditions.

Studies[5–9] carried out during the past two decades allowed one to understand and verify some details of such flows for certain values of determining parameters. A strong influence of the turbulence level in the wake on the process of its interaction with the boundary layer of a flat surface was found by Zhou and Squire.[10,11] From the computational viewpoint one can see that the most severe problems arise in the initial section of interaction where the flow regions having a negative turbulent viscosity are formed.

Some studies[12–14] were performed for configurations used in aircraft engineering, and the results are rather specific. A number of papers (e.g., Refs. 15, 16, and others) are devoted to experimental investigation of aerodynamic forces and moments (e.g., lift and rolling moment) acting upon a schematized flying vehicle that is entrained into the wake of an upstream aircraft. The data obtained were used to construct an aerodynamic model that allowed evaluation of the interference between the upstream and downstream flying vehicles.

In addition to this, it should be emphasized that some of the papers just referenced were concerned with gaining an understanding of the effect of the wake from an wing slat on the boundary-layer flow on the wing surface immediately downstream of the slat; thus, part of the initial boundary layer was not in the wake flow, and the wake gradually merged with the boundary layer. Also in some of studies care was taken to ensure that the presence of the wake-producing airfoil did not change the pressure field.

Unlike the papers just cited, the initial flows (wake and boundary layer) in the present study are formed in the flow around fully identical, comparatively thin symmetric airfoils located in tandem, which can change their positions both in the streamwise and crosswise directions. Thus, to study the structure and properties of an interacting flow in the framework of a simple model approach is possible when the relative positions of the wake and boundary layer are changed. This is of vital importance because these changes lead to a significant amplification or attenuation of the interaction intensity up to complete vanishing of the interaction process. However, in actual practice this process can be complicated by vortices shed from the wing tip. In the approach used here, this influence is deliberately eliminated so that the problem is not complicated by additional effects. Thus, the relative simplicity of the models used and their practical validity offer an opportunity to study the basic regularities of the development of such flows, which, in turn, can form the basis for constructing a physical flow model.

Some comments should be made concerning the term *interaction* used here. Obviously, this term can be used when two (or more) independent hydrodynamic flowfields (structures, non-uniformities, etc.) start to affect each other (as, for example, the interaction between a shock wave and a boundary layer). In principle, such a situation arises in the present study when the peripheral part of an asymmetric turbulent wake falls on a developed boundary layer of a wing immediately downstream. When the wing is located in the central part of the wake, it is probably more reasonable to say that the boundary layer on such a wing is formed under wake flow conditions with inherent properties. Nevertheless, we will conventionally use the term interaction although in most cases we deal with an asymmetric nonuniform turbulent shear flow around an airfoil.

II. Experimental Conditions and Procedure

The wind tunnel used for these experiments was the closed-return low-turbulence wind tunnel. The tunnel is driven by an axial fan and powered by a 0.6-MW dc motor. The settling chamber contains 10 screens with a special filter mounted on the first screen. The contraction reduces the octahedral cross section of the settling chamber to the square cross section of the test section with the fillets in the corners and has a contraction ratio 17:1. The test section has a cross section of 1×1 m^2 and a length of 4 m. The streamwise velocity fluctuations are less than 0.06% at a velocity $\bar{u}_\infty$ of 25 m/s for the present experiments.

The model under study consists of two identical unswept rectangular airfoils (upstream and downstream) located in tandem in the test section (Fig. 1). The construction allows various wing positions in the streamwise x and crosswise y directions and various angles of attack α within $\alpha = \pm 40$ deg. The models were mounted vertically to avoid problems with model bending from its weight and for convenience of measurements the models spanned the tunnel height. Each of the wings had a Joukowskii-type symmetrical airfoil section with a chord $c = 257$ mm, whole span 970 mm, and relative thickness $t/c = 0.07$. Static-pressure orifices 0.35 mm in diameter were located at the both sides of the wing along its central chord.

The choice of the wing geometry and its relative thickness was conditioned by two basic considerations. First, the known property of hysteresis of steady total and distributed characteristics does not manifest itself in the flow around comparatively thin airfoils.[17] Second, the aerodynamic characteristics become independent of the Reynolds number,[18] which is important for identification of the general features of the flow under study.

To reduce the tip vortex intensity and increase the effective aspect ratio of the wing AR_{eff}, the model was equipped with aerodynamic end plates made as ellipses whose major axis is 1.5 of the wing chord. The distance l between the end plates in the wing span direction is 771 mm, which corresponds to the wing aspect ratio $AR = 3.0$. However, following the results of Krassilschikoff,[19] the actual aspect ratio is determined from the formula

$$AR_{\text{eff}} = AR[1 + 1.66\,(h/l)]$$

where h is the end-plate height. Thus, in our case AR_{eff} was equal to 3.83.

A three-dimensional flow with longitudinally developing vortices is formed in the regions of junction of the end plates and the wing surface, which are typical corner configurations.[20] To reduce the adverse effect of these vortices on the main flow region, we used fillets whose geometry was chosen on the basis of data of Kornilov and Kharitonov.[21] Preliminary experiments showed that the flow around such a wing is planeparallel and is essentially similar to the flow around a wing with an infinite aspect ratio. Visualization of the limiting streamlines did not reveal any flow singularities, such as node or saddle points, foci, etc. Thus, the efficiency of the fillets used was confirmed.

The test angle of attack range was -7.5–18 deg in increments of 2–2.5 deg. The actual angle of attack of the wing was established using a Vernier incidence scale with an optical cursor having an error not exceeding 0.25 deg. The initial position of the wing corresponding to a zero angle α was determined on the basis of a calibration dependence $(P_W - P_L)/q_\infty = f(\alpha_{\text{sc}})$, which was verified for each set of experiments. Here, $(P_W - P_L)$ is the pressure difference measured in the points characterized by an equal x coordinate at the windward and leeward sides of the model, and α_{sc} is the angle of attack of the model registered on a scale.

The value of dynamic pressure q_∞ was controlled using the difference between the total and static pressure registered by a Pitot–Prandtl tube mounted at a distance of about four chord lengths upstream of the model. The freestream velocity upstream of the model

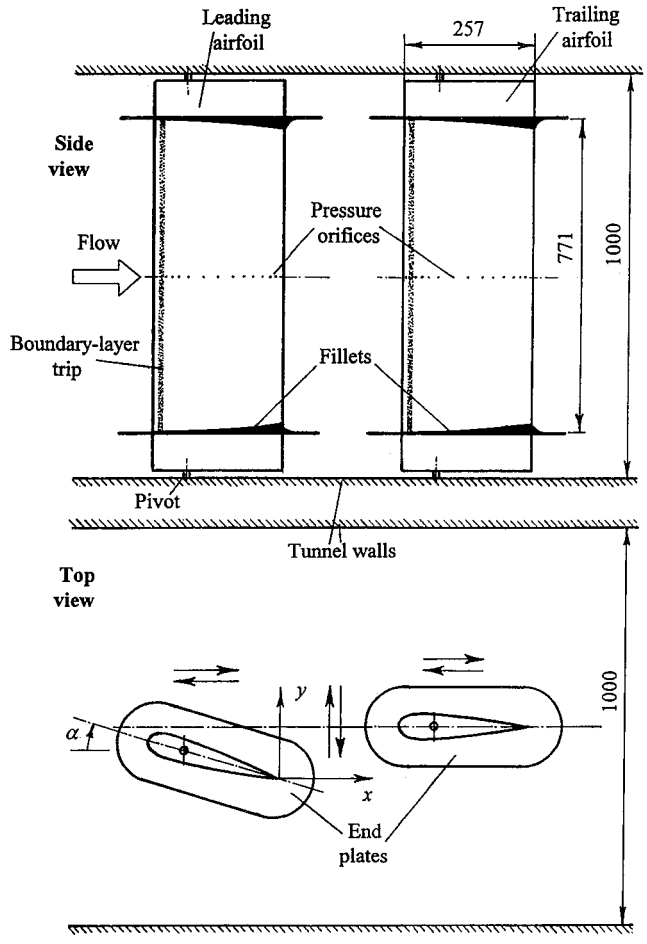

$(x^*/c)\times10^3$	2	7	15	27	42	60	81	106	133	163	195	230	266	305
$(y^*/t)\times10^3$	67	133	196	256	311	359	402	439	464	484	496	500	496	486
$(x^*/c)\times10^3$	387	473	561	647	730	769	806	840	872	900	926	948	967	981
$(y^*/t)\times10^3$	445	385	313	238	168	137	108	83	62	44	31	21	14	12

Fig. 1 Schematic of the model and tested airfoil profile coordinates. (Not to scale; all dimensions in millimeters.)

was kept constant at $\bar{u}_\infty = 25$ m/s, which yielded a Reynolds number based on airfoil chord $Re_c = 4.28 \times 10^5$ ($Re_1 = 1.66 \times 10^6$ m^{-1}).

The static pressure on the model surface was measured by pressure orifices at various positions in the streamwise direction and changing angle of attack of the airfoil. The pressure taps were connected by a device similar to a Scanivalve to a DISA micromanometer.

To carry out the boundary layer and wake measurements, a manually controlled traverse gear having three degrees of freedom was used. The traverse gear provided linear movements with an accuracy of 0.01 mm (precise scale) and 0.1 mm (rough scale) in the y direction and with an accuracy of 0.5 mm in the x direction and also the angular rotation in the xy plane with an accuracy of 0.5 deg.

The mean velocity and the streamwise component of velocity fluctuations were measured using a DISA 55M hot-wire constant temperature anemometer. The arrangement included a 55M10 hot-wire bridge with a 55D10 linearizer connected to its output. The constant component of the linearized signal corresponding to the mean flow velocity $\bar{u}$ was measured using a 55D31 digital dc voltmeter. The variable component of the signal corresponding to the rms value of the streamwise velocity component $\sqrt{u'^2}$ was filtered by a 55D25 auxiliary unit and measured by a 55D35 rms voltmeter. As a primary-measuring transducer, a miniature hot-wire probe with a single sensor made of tungsten wire with diameter of 5 μm and active length 1.2 mm was used. In the course of measurements, the probe wire was oriented perpendicular to the freestream velocity vector.

The experiments were carried out in two stages. During the first stage, the characteristics of the components of the interacting flow, namely, an isolated wake and an isolated boundary layer, were analyzed under naturally developing conditions. During the second stage, the boundary layer on both wings was artificially tripped. This was done using a strip of sandpaper 12 mm long and 0.6 mm thick glued along the wing span on both its sides at a distance of about 5% of the chord from the leading edge. Such an approach assumed that a trip chosen would still produce a fully developed turbulent boundary layer over the flow surface, and the boundary layer would attain equilibrium some reference trip thicknesses downstream of its position.

For the downstream wing to be in the wake influence zone, the upstream wing should be mainly moved in the positive direction of the y axis (to the left-side wall of the wind tunnel). In this case the generated wake had a general direction from the left to the right tunnel wall (looking downstream) occupying the flow core region. Therefore, we hope that the wake flow interference with the boundary layer on the tunnel walls is negligible.

The main measurements were performed in 14 stations along the wake in the range from $x/c = 1.004$ (near the wing trailing edge) to $x/c = 2.543$ (far wake) and in eight cross sections in the boundary layer of the downstream wing within $x/c = (0.195 \div 0.962)$.

A detailed discussion of the measurement error for the different techniques used in these experiments is summarized in Table 1. Let us only note that for variables C_p, T_∞, q_∞, $\bar{u}$, $\bar{u}_\infty$, and $\sqrt{u'^2}$ Table 1 gives the random measurement error normalized to their maximum values observed in experiments. It does not seem possible to present the normalized measurement errors in a more suitable form because they vary significantly over the height of the region under study. The sign of averaging of some variables (C_p, etc.) is omitted for simplicity.

Table 1 Estimates of measurement errors

Measured variable	Method of measurement	Measurement error	Remark
Angle of attack of airfoil	Vernier incidence scale	0.25 deg	——
Distance from wall	Traverse gear	0.01 mm	Precise linear scale
		0.1 mm	Rough linear scale
Streamwise distance	Traverse gear	0.5 mm	——
C_p	TSAGI micromanometer and DISA micromanometer	±0.3%	——
T_∞	Electronic thermometer	±1%	——
q_∞	DISA micromanometer	±0.25%	——
$\bar{u}_\infty$	DISA micromanometer and lab. equipment to measure air density ρ	±0.5%	——
$\bar{u}$	Hot wire	±0.5%	——
$\sqrt{\overline{u'^2}}$	Hot wire	±2%	——

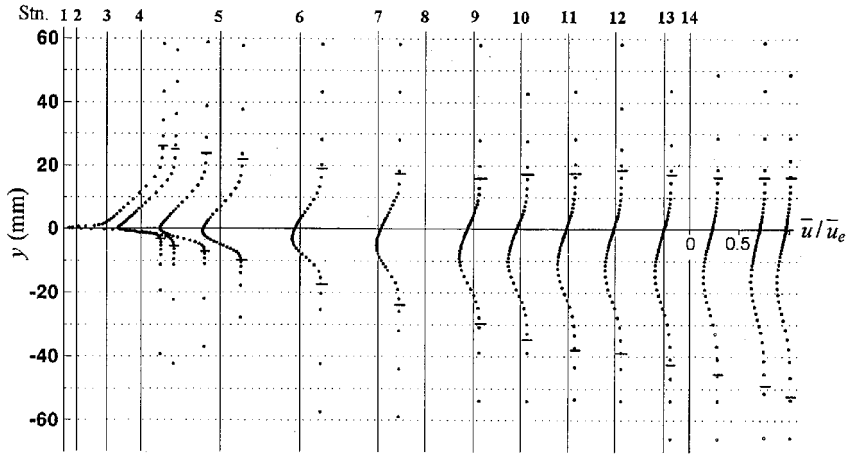

Fig. 2 Streamwise mean velocity profiles in the wing wake at $\alpha = 7.5$ deg. Values of chordwise location x/c: 1, 1.004; 2, 1.037; 3, 1.111; 4, 1.196; 5, 1.391; 6, 1.586; 7, 1.780; 8, 1.897; 9, 2.014; 10, 2.130; 11, 2.247; 12, 2.364; 13, 2.480; and 14, 2.543.

III. Results and Discussion

The objective of the first stage of the study was an analysis of the state of the boundary layer and the wake behind an airfoil under naturally developing conditions. It was essential to find the range of the angle of attack where the flow around the airfoil is attached to avoid complicating the problem by additional influences of separation effects. The results obtained are exactly as expected and just show that for the cases no more than 9 deg the flow over the airfoil is attached. This circumstance was the basis for choosing the test flow regime for subsequent experiments, which involved an angle of attack of $\alpha = 7.5$ deg. In the course of subsequent measurements, the time-averaged parameters of the flow and turbulence characteristics of an isolated wake and boundary layer on the airfoil at angles $\alpha \leq 7.5$ deg were analyzed in detail. Similar to Cousteix and Pailhas[3] and Cousteix et al.[4] for the wake behind a swept wing, a natural transition to turbulence at the leeward side of the model takes place. Therefore, at $\alpha = 7.5$ deg the boundary layer is turbulent beginning from the leading edge. The level of turbulent velocity fluctuations at the windward side of the model is a transitional flow, at least, at $\alpha = 7.5$ deg. This is also confirmed by analysis of other characteristic quantities: mean velocity isolines and isolines of the streamwise component of velocity fluctuations in the boundary layer and in the wake itself. Obviously, the ambiguous state of the flow behind the windward and, hence, leeward sides of the wing can alter significantly the pattern of the wake interaction with the boundary layer of a downstream wing. Therefore, all subsequent experiments were carried out using artificial tripping of the boundary layer on the both sides of the wing.

A. Characteristics of the Isolated Wake

Figure 2 is a plot of the mean velocity profiles $\bar{u}/\bar{u}_e = f(y)$ at 14 stations along the wake produced by an airfoil installed at an angle $\alpha = 7.5$ deg. In the following $y = 0$ coincides with the plane passing through the trailing edge of the wing parallel to the longitudinal axis of the wind tunnel. The upper and lower boundaries of the wake shown by horizontal lines are defined as distances toward the y axis where the linear character of the mean velocity distribution across the wake begins. (The linearity of $\bar{u}/\bar{u}_e$ is caused by a changeability of velocity of potential flow in this region and has the same sense as for a flow past a curved wall.)

There is an explicit asymmetry in the mean velocity distribution with respect to $y = 0$ in the near wake for the results plotted in Fig. 2 (stations 1–3). That asymmetry is caused by a significant difference of the boundary-layer formation at the suction and pressure sides of the wing. As the x/c coordinate increases, a tendency to symmetrization and flattening of the profile $\bar{u}/\bar{u}_e = f(y)$ is observed. Typically, the deviation of the wake axis y_0 from the value $y = 0$ determined by the position of the minimum velocity line in the profile $\bar{u}/\bar{u}_e = f(y)$ has a constant value roughly equal to 2.5 deg. An exception is only the flow region $1.0 \leq x/c \leq 1.1$ (near wake) whose behavior is more complicated. Besides, this is fairly well validated by the distribution of equal velocity lines $\bar{u}/\bar{u}_e = \text{const}$ (Fig. 3), where the velocity minimum does not change within the mentioned region.

Analysis of regularities of the mean velocity evolution across the wake is of interest. For this purpose self-similar coordinates are used to describe the normalized velocity defect $(\bar{u}_e - \bar{u})/(\bar{u}_e - \bar{u}_{\min})$ in the wake produced by a transverse-positioned cylinder. The results of this approach are illustrated in Fig. 4. The y coordinate was measured from the position of the wake axis, and $y_{0.5}$ corresponds to the value of y where the velocity defect is half of the maximum value. In a wake two values of $y_{0.5}$ can be determined. In this paper $y_{0.5}$ was defined as $y_{0.5} = (y_{0.5[+]} + y_{0.5[-]})/2$. The change of $y_{0.5}$ along the wake correlates satisfactorily with the empirical formula $y_{0.5} = 0.693\sqrt{x}$ derived by Marumo et al.[22] for an isolated circular cylinder.

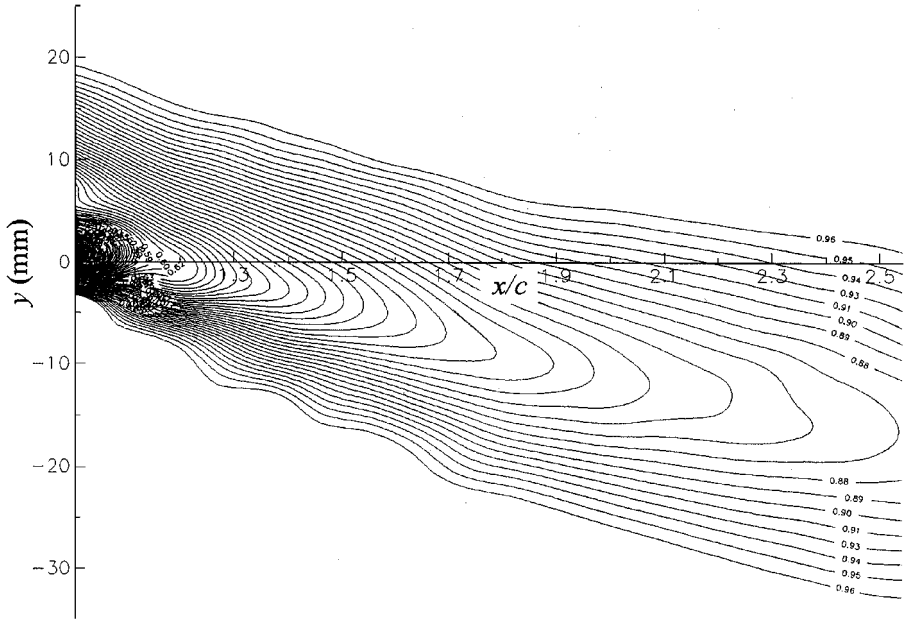

Fig. 3 Streamwise mean velocity contours $\bar{u}/\bar{u}_e$ = const in the wing wake at $\alpha = 7.5$ deg.

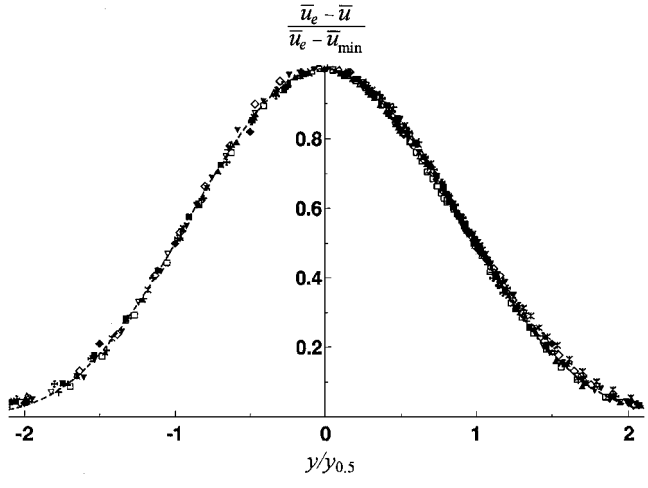

Fig. 4 The shape of self-similar streamwise mean velocity profile in the wing wake at $\alpha = 7.5$ deg. Values of chordwise location x/c: △, 1.196; ▲, 1.391; □, 1.586; ■, 1.780; ▽, 1.897; ▼, 2.014; ◇, 2.130; ✠, 2.247; ×, 2.364; ∗, 2.480; and ♦, 2.543; - - - -, exponential function of Ref. 23: $(\bar{u}_e - \bar{u})/(\bar{u}_e - \bar{u}_{\min}) = \exp[-0.637(y/y_{0.5})^2 - 0.056(y/y_{0.5})^4]$.

The profiles measured in a clearly asymmetric wake have a self-similar character (except for the near wake region mentioned early) and are readily approximated by the exponential function

$$\frac{\bar{u}_e - \bar{u}}{\bar{u}_e - \bar{u}_{\min}} = \exp\left[-0.637\left(\frac{y}{y_{0.5}}\right)^2 - 0.056\left(\frac{y}{y_{0.5}}\right)^4\right]$$

suggested by Wygnanski et al.[23] (dashed line) for the wake flow behind a circular cylinder.

Now consider some flow features in an isolated wake behind the wing. Wygnanski et al.[23] found that in the far wake formed by symmetric generators of different shapes the dimensionless half-width of the wake is a function of velocity defect and has an universal form, as follows:

$$\delta_f^{**} \big/ y_{0.5} = f[(\bar{u}_e - \bar{u}_{\min})/\bar{u}_e]$$

where δ_f^{**} is the momentum thickness in the asymptotic wake region, which is usually taken in a far station of the wake.[24] Using such a representation in Fig. 5 yields a good correlation of all of the data, including those of Ref. 23 (dashed band), as a simple linear

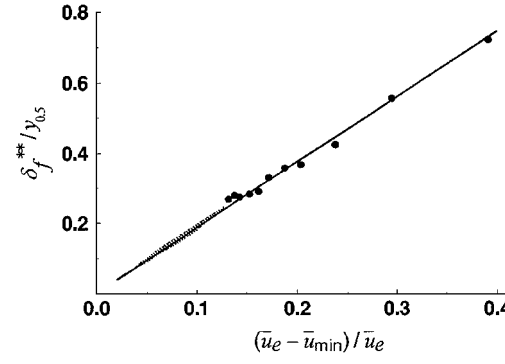

Fig. 5 The dependence of $\delta_f^{**}/y_{0.5}$ as a function $(\bar{u}_e - \bar{u}_{\min})/\bar{u}_e$: ●, present results; the shaded region shows the boundaries of experimental values according to Ref. 23 for various wake generators.

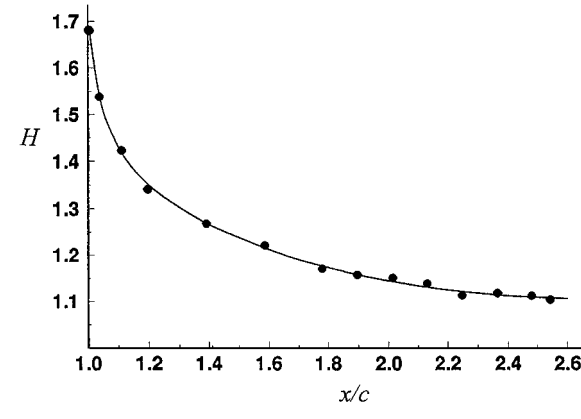

Fig. 6 Variation of shape factor along the wing wake at $\alpha = 7.5$ deg.

expression. Moreover the results of the present work cover not only the far wake flow, but also the flow region located closer to the trailing edge of the wing. Thus, it seems probable that the dependence suggested in Ref. 23 has a universal character.

The evolution of the integral characteristics of the wake flow can be presented by the change of the shape factor $H = \delta^*/\delta^{**}$ along the streamwise coordinate x/c plotted in Fig. 6. Here

$$\delta^* = \int_{-\infty}^{\infty}\left(1 - \frac{\bar{u}}{\bar{u}_e}\right)\mathrm{d}y, \qquad \delta^{**} = \int_{-\infty}^{\infty}\frac{\bar{u}}{\bar{u}_e}\left(1 - \frac{\bar{u}}{\bar{u}_e}\right)\mathrm{d}y$$

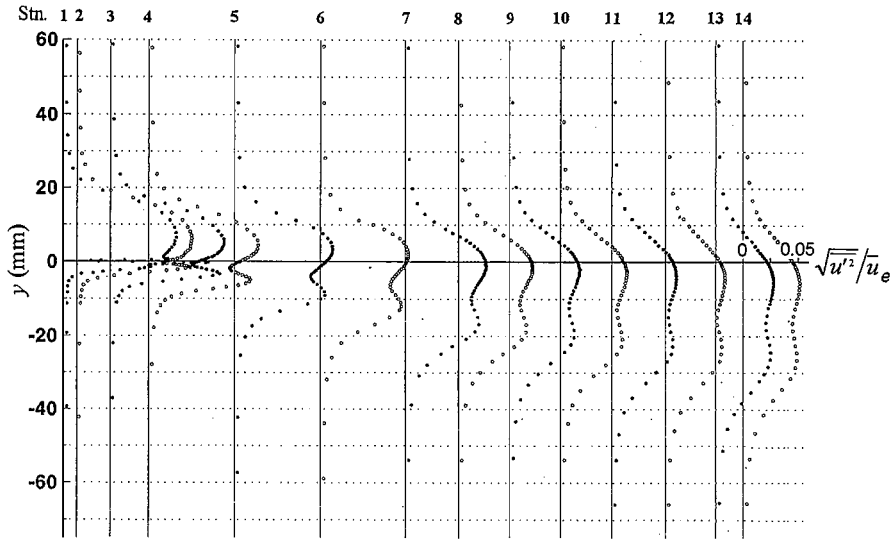

Fig. 7 Streamwise rms velocity fluctuation profiles in the wing wake at $\alpha = 7.5$ deg. Designations are the same as in Fig. 2.

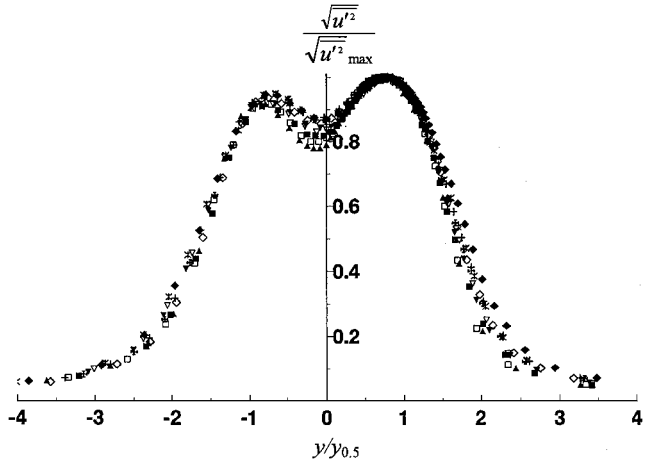

Fig. 8 The normalized streamwise turbulent normal stresses distribution across the wake at $\alpha = 7.5$ deg. Values of chordwise location x/c: ▲, 1.391; □, 1.586; ■, 1.780; ▽, 1.897; ▼, 2.014; ◊, 2.130; ✠, 2.247; ×, 2.364; ∗, 2.480; and ♦, 2.543.

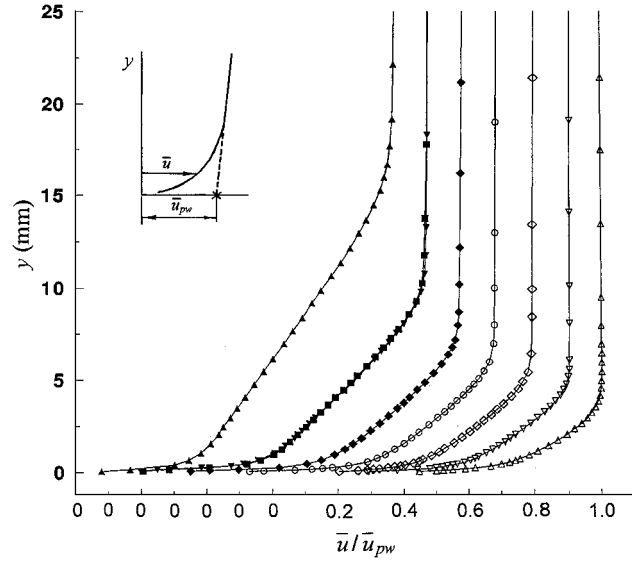

Fig. 9 Boundary-layer streamwise mean velocity profiles at $x/c = 0.962$ on the windward side (open symbols) and leeward side (closed symbols) of an isolated wing. Values of angle of attack: ○, 0 deg; ◊ and ♦, 2.5 deg; ▽, ▼, and ■, 5 deg; and △, ▲, 7.5 deg.

are the displacement thickness and momentum thickness determined from the streamwise component of the wake velocity vector. Near the trailing edge of the wing ($x/c = 1.004$), the value of H is 1.68, which is somewhat higher than its commonly observed value in gradient free turbulent boundary layers. Obviously, this behavior is caused by the influence of the adverse pressure gradient on the leeward side of the wing. As x/c increases, the shape factor H rapidly decreases, but it is clear that the asymptotic character of this dependence extends to considerably larger distances along the wake.

Figure 7 shows the profiles of the streamwise rms component of velocity fluctuations $\sqrt{\overline{u'^2}}/\bar{u}_e = f(y)$ along the wake. Considerable flow asymmetry is evident in the near wake, which vanishes gradually downstream. On the whole, the profiles possess the features of a turbulent boundary layer formed under the conditions of a gradient flow on the wing. Indeed, at negative values of y, the profile has a maximum (peak) around $y = 0$, and this resembles a corresponding profile on a flat plate; at positive values of y, the maximum in the distribution $\sqrt{\overline{u'^2}}/\bar{u}_e = f(y)$ is shifted upward, which reflects the existence of an adverse-pressure gradient on the leeward side of the wing. The lines of equal values $\sqrt{\overline{u'^2}}/\bar{u}_e = \text{const}$ in the wake especially in the flow region $1.0 \le x/c \le 1.1$ are an additional support to this statement.

The data on distribution of turbulent velocity fluctuations in the wake behind a symmetric generator indicate that each wake is approximately self-similar.[23] However, this process depends on geometry of the wake generator. In this connection it is of interest to consider analogous distributions in self-similar coordinates for a considerably asymmetric wake behind an airfoil (Fig. 8). Here, $\sqrt{\overline{u'^2}}_{\max}$ is the maximum value of the streamwise component of velocity fluctuations in the profile $\sqrt{\overline{u'^2}}/\bar{u}_e = f(y)$. Although the scatter of the values of $\sqrt{\overline{u'^2}}/\sqrt{\overline{u'^2}}_{\max}$ is large (see the region $-0.8 \le y/y_{0.5} \le 0.1$) and it has a systematic rather than random character, the profiles presented appear to have a form close to a self-similar behavior. Thus, apart from some specific features, an asymmetric turbulent wake behind an airfoil has a certain similarity with known types of flow.

B. Characteristics of the Isolated Boundary Layer

Figure 9 shows the mean velocity profiles on the windward and leeward sides of the wing ($x/c = 0.962$) for various values of the angle α as a function $\bar{u}/\bar{u}_{\text{pw}} = f(y)$. Here, $\bar{u}_{\text{pw}}$ is the potential flow velocity on the wall (Refs. 25, 26) whose essence can be understood from the inset figure. On the whole the data presented have nothing unexpected and correlate with the known concepts of the flow around a wing at incidence (see, for example, Refs. 27–29, and others). In particular, the just-mentioned growth of the adverse-pressure

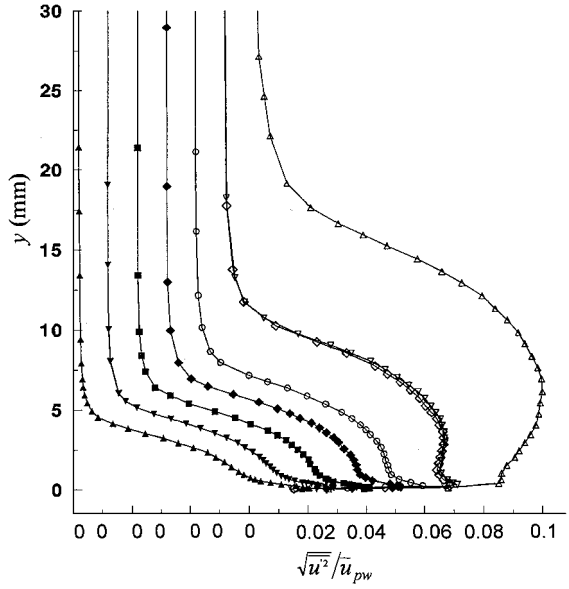

Fig. 10 Boundary-layer rms streamwise velocity fluctuation profiles at $x/c = 0.962$ on the windward side (closed symbols) and leeward side (open symbols) of an isolated wing. Values of angle of attack: ♦, 0 deg; ○ and ■, 2.5 deg; ▽, ◇, and ▼, 5 deg; and △ and ▲, 7.5 deg.

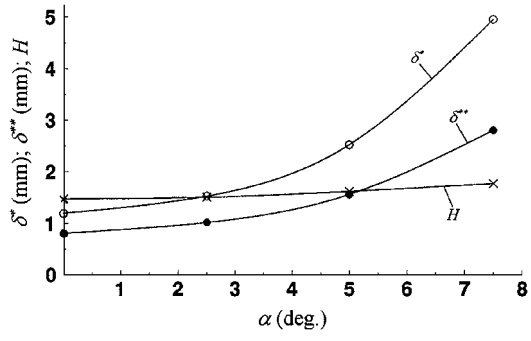

Fig. 11 Variation of boundary-layer integral parameters on the leeward side with angle of attack ($x/c = 0.962$).

gradient on the leeward side of the wing with increasing α favors a reduction of profile fullness (closed symbols). Naturally, a reverse tendency is observed on the windward side of the wing (open symbols).

The profiles of turbulent velocity fluctuations (Fig. 10) on the windward side (closed symbols) are characterized by the maximum $\sqrt{u'^2}/\bar{u}_{\rm pw}$ near the wall resembling a corresponding profile on a flat plate. On the leeward side (open symbols), on the contrary, the growth of the angle α rapidly shifts the characteristic maximum from the wall and increases simultaneously the amplitude of fluctuations, which is also typical for this type of the flow.

Some idea about the integral characteristics of the boundary layer δ^*, δ^{**}, and H on the leeward side of the model with varied α is presented in Fig. 11, which illustrates the results of measurements in the cross section $x/c = 0.962$. Here, the integral thicknesses δ^* and δ^{**} have the form that is generally applied for the flow past a curved wall[25] where as a reference velocity is used the potential flow velocity $\bar{u}_p$ (see the inset to Fig. 12). As expected, the value of H at $\alpha = 7.5$ deg is close to the corresponding value obtained in the wake near the trailing edge of the wing ($x/c = 1.004$).

Now consider in more detail the boundary-layer characteristics at $\alpha = 0$ deg because the study of the interacting flow was carried out for the downstream wing at zero incidence. The mean velocity profiles $\bar{u}/\bar{u}_{\rm pw} = f(y)$ measured at different dimensionless distances x/c from the leading edge of the wing contain nothing unexpected. It is more important that the distribution of mean velocities in the boundary layer plotted in the terms of the variables $\bar{u}/\bar{u}_p = f(y/\delta^{**})$ has a self-similar character (Fig. 12). An exception is only the first

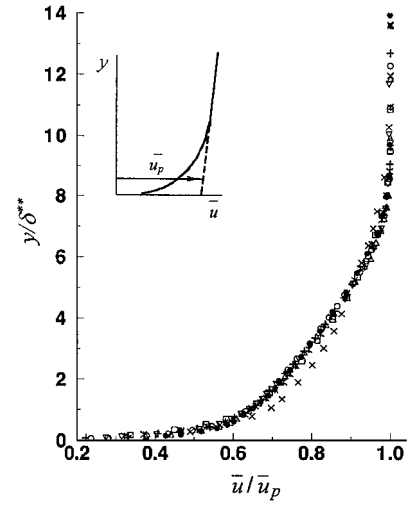

Fig. 12 Nondimensional boundary-layer streamwise mean velocity profiles at zero angle of attack. Values of chordwise location x/c: ×, 0.195; □, 0.311; ∗, 0.428; ●, 0.545; ▽, 0.661; +, 0.778; △, 0.895; and ○, 0.962.

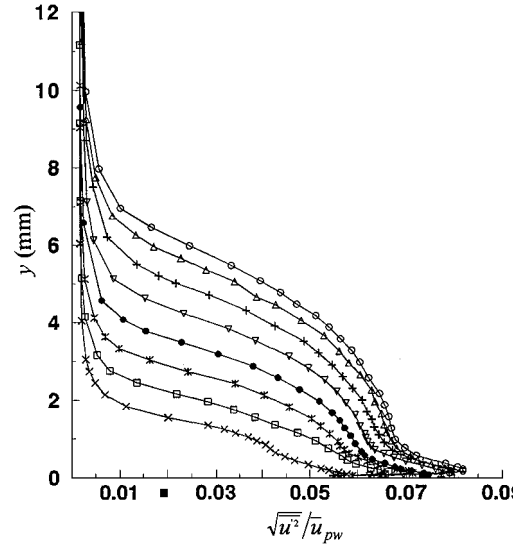

Fig. 13 Boundary-layer streamwise rms velocity fluctuation profiles at zero angle of attack of the wing. Designations are the same as in Fig. 12.

cross section ($x/c = 0.195$), which is caused by the formation of a nonequilibrium flow region behind the boundary-layer trip. Similar behavior is also noticeable in plots of turbulent velocity fluctuations $\sqrt{u'^2}/\bar{u}_{\rm pw}$ (Fig. 13) as reduced fluctuations in the near-wall flow region at the first measurement cross section.

The chordwise distribution of integral characteristics of the boundary layer δ^*, δ^{**}, H, and C_f for the same experimental conditions are presented in Fig. 14. The local skin-friction coefficient C_f was determined from the well-known empirical correlation of Ludwieg and Tillmann:

$$C_f = 0.246 \cdot 10^{-0.678 \cdot H} \cdot Re_{\delta^{**}}^{-0.268}$$

based on the use of experimental values of H and δ^{**}. Interestingly, the shape factor H remains nearly constant along the model. This behavior can be explained as follows. A decrease of H along the model is observed in a gradient-less turbulent boundary layer. On the other hand, the presence of an adverse pressure gradient favors the growth of H. Obviously, the present pressure gradient is such that the shape factor is kept nearly constant as x varies.

C. Characteristics of the Interacting Flow

The flow characteristics for conditions when a turbulent wake interacts with a boundary layer were measured at the same cross

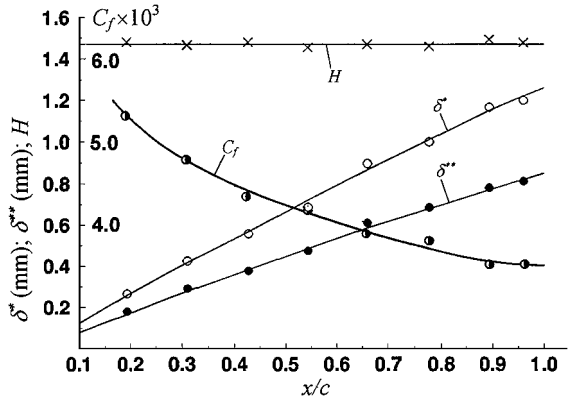

Fig. 14 Chordwise variation of boundary-layer integral parameters and local skin-friction coefficient at zero angle of attack of the wing.

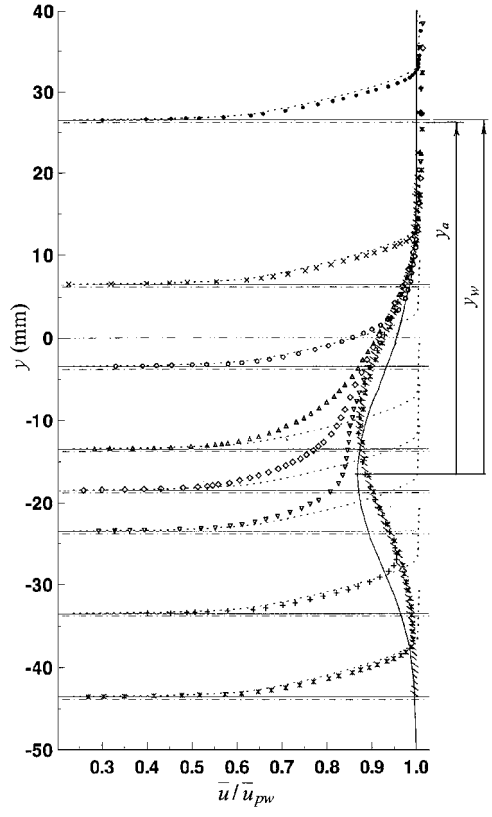

Fig. 15 Streamwise mean velocity profiles at $x/c = 0.962$ and various position of the wing across the wake (symbols) as compared with corresponding boundary-layer profiles for isolated wing (· · · ·) and wake (——); – · –, wing trailing-edge position.

sections as for isolated flow around the wing. Most of the experiments considered conditions when the downstream wing was located in the wake flow region with coordinates $1.58 \le x/c \le 2.58$. The following measurement procedure was used. The downstream wing was mounted at a given distance y_a across the wake, and measurements were performed in eight cross sections along the wing. (Here y_a is the distance from the wake axis to the wing chord at an examined cross section x/c). Naturally, depending on the y_a coordinate, the wing was in different flow regions with mean and fluctuating charateristics either weakly or strongly changing in the streamwise direction.

As an example, Figs. 15 and 16 show the distributions of the mean velocity $\bar{u}/\bar{u}_{\rm pw}$ and the streamwise component of velocity fluctuations $\sqrt{\overline{u'^2}}/\bar{u}_{\rm pw}$ at the cross section $x/c = 0.962$ for various y_a. For simplicity the mean and fluctuating velocity profiles for isolated wakes and boundary layers are shown by solid and dashed lines, respectively. The data presented here refer to the last measurement cross section where the wing thickness is small. In this connection

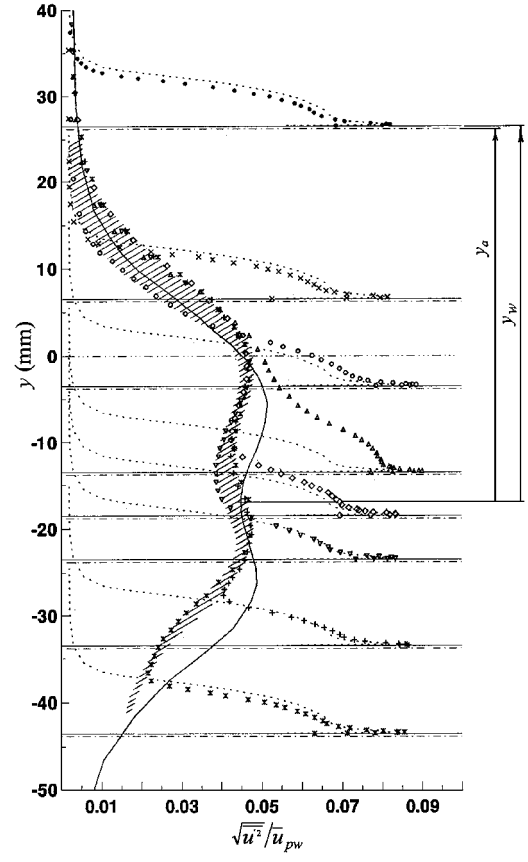

Fig. 16 Streamwise rms velocity fluctuation profiles at $x/c = 0.962$ and various position of the wing across the wake (symbols) as compared with corresponding boundary-layer profiles for isolated wing (· · · ·) and wake (——). Other designations are the same as in Fig. 15.

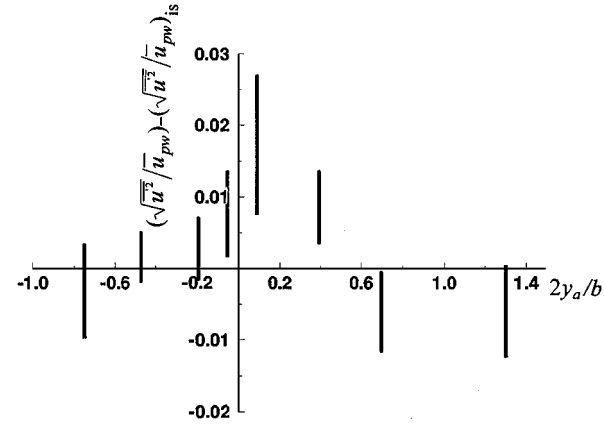

Fig. 17 Histogram showing the flow regions with favorable and unfavorable interference on the wake width. ($x/c = 0.962$.)

the line coinciding with the wing chord (dash-dotted line) is located near the point (conventionally shown by a line) that characterizes the profile coordinate in a given cross section.

The following typical features of the flow under study should be noted:

1) If the wing is located at the wake periphery ($y = 26.2$, 6.2, and -43.8 mm), a certain increase in mean velocity is observed simultaneously with a decrease in the level of turbulent fluctuations, as compared with the case of an isolated flow. The latter can be proved by considering a conventional histogram (Fig. 17) that shows the presence of flow regions with favorable and adverse interference at various relative position of the wing $2y_a/b$. The vertical sections indicate the difference between the turbulent velocity fluctuations of the interacting flow and the corresponding values for the flow around an isolated wing. Data on the boundary layer height are presented up to an external flow region where a so-called generic

profile is observed (see the following). When the wing is located near the upper ($2y_a/b \approx 1$) or lower ($2y_a/b \approx -1$) wake boundary, flow regions with favorable interference prevail {the difference $[(\sqrt{\overline{u'^2}}/\bar{u}_{pw}) - (\sqrt{\overline{u'^2}}/\bar{u}_{pw})_{is}]$ is negative}. This behavior can be explained as follows. First, with the flow around the wing under study being assumed similar to the flow around some body under the influence of an increased freestream turbulence, some useful considerations can be noted. In particular, increasing the velocity profile fullness on a flat surface with increasing the freestream turbulence is well known.[30] Concerning the streamwise component of velocity fluctuations, these authors emphasize a conservative character of distribution of this quantity near the wall. In principle, such a tendency is also observed in the present tests (Fig. 16). At the same time, inside the boundary layer Dyban and Epik[30] noticed only an increase of $\sqrt{\overline{u'^2}}/\bar{u}_e$ toward the wall; the lower the freestream turbulence, the higher this increase. (Unlike $\sqrt{\overline{u'^2}}/\bar{u}_e$, the component $\sqrt{\overline{v'^2}}/\bar{u}_e$ can decrease as the freestream turbulence increases.) Second, the downstream airfoil is in a downwash field. Clearly the downwash changes one surface into a suction surface and the other into a pressure surface. Therefore one would expect the downwash effect to decrease the longitudinal pressure gradient and as a consequence to attenuate the turbulent fluctuations on the examined surface of the downstream airfoil.

2) For any value of y_a, the profile of the mean velocity and, hence, the streamwise component of velocity fluctuations in the outer region of the interacting flow follows the isolated wake profile. Within a certain uncertainty band (dashed band), it is possible to identify in this region a typical profile that unifying for all values of y_a, called a *generic* profile. This generic profile is shifted with respect to the isolated wake profile toward the positive values of y at a distance Δy. Analysis shows that the value of the dimensionless ratio $\Delta y/c$ for identical x/c smoothly decreases with increasing distance Δx between the upstream and downstream airfoils. It can be expected, however, that the asymptotic behavior of this dependence can be traced downstream over a large distance.

3) The distribution of the analyzed quantities in the intermediate flow region has a more complicated character. When approaching the wake axis, the profiles of both the mean velocity and turbulent fluctuations deviate from the corresponding distributions typical of an isolated boundary layer and acquire gradually the features of an isolated wake profile. It is worth noting that the level of turbulent fluctuations in the generic profile decreases compared to corresponding values in an isolated wake. These features are observed for all values of the x/c coordinate. When approaching the leading edge of the wing, the difference in the level of turbulent fluctuations of $\sqrt{\overline{u'^2}}/\bar{u}_{pw}$ in the generic profile and isolated wake increases noticeably. Similar measurements performed when the position of downstream airfoil was changed along the wake (though within narrow limits) showed that this effect is conserved. The mentioned early complex character of distributions of the time-averaged and fluctuating flow quantities inside the interaction region does not yet provide simple correlation functions for their generalization.

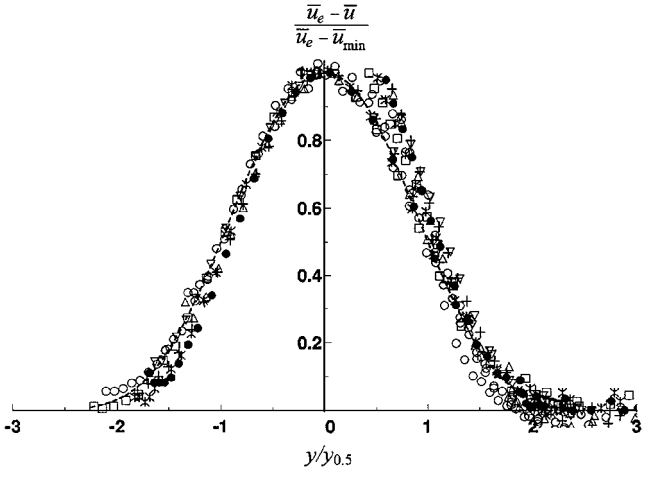

Fig. 18 Shape of self-similar mean velocity profile in the external part of interacting shear flow. Values of chordwise location x/c: □, 0.311; ∗, 0.428; ●, 0.545; ▽, 0.661; +, 0.778; △, 0.895; and ○, 0.962. Other designations are the same as in Fig. 4.

As far as the outer flow region is concerned, the previous features laid the basis for generalizing the data on the mean velocity distribution in self-similar coordinates. Data obtained are presented in Fig. 18. The results of measurements at eight cross sections along the wing for its seven positions y_a across the wake are shown. (For simplicity, the normalized velocities for a particular value of x/c are designated by one symbol irrespective of the value of y_a.) Although the scatter of experimental data is large, all of the data correlate as a single curve (dashed line) used to describe the normalized profile of velocity defect in the wake behind a transverse-positioned cylinder. This means that the outer region of the interacting flow under study can be approximately described in the framework of the known model.

IV. Conclusions

An experimental study of the interaction of an asymmetric two-dimensional wake produced by a symmetric airfoil at incidence with a boundary layer formed on a similar airfoil immediately downstream was carried out for incompressible flow. On the basis of this work, several conclusions may be drawn:

1) The normalized profile of velocity defect in an asymmetric isolated wake can be easily described in the framework of the well-known correlations valid for a wake flow behind a transverse-positioned cylinder. One can also argue that the profile of rms fluctuations of the streamwise velocity component on a significant distance along the wake can be roughly described using self-similar coordinates.

2) A self-similar character of the mean velocity profiles in the boundary layer on an isolated wing, except for the first measurement cross section, gives grounds to believe that the shear flow is in an equilibrium state on the larger part of the model. This fact seems important because the additional flow features caused by nonequilibrium, separation, etc., could only complicate the interaction process.

3) Some increase in the mean velocity was observed simultaneously with suppression of turbulent velocity fluctuations in the interacting flow, as compared with an isolated flow, when the airfoil is located in the peripheral part of the wake. A similar effect was also observed in the outer region of the interacting flow when the airfoil is located in the central part of the wake.

4) Normalized profiles of velocity defect in the outer region of the interacting flow can be roughly described by simple correlations traditionally used for a wake flow behind a transverse-positioned circular cylinder.

Acknowledgment

The authors would like to express their sincere thanks to J. Cousteix from ONERA–Toulouse for his attention to this problem.

References

[1] Mabey, D. G., "Beyond the Buffet Boundary," *Aeronautical Journal*, Vol. 77, No. 748, 1973, pp. 201–215.

[2] Clauser, F. H., "Turbulent Boundary Layers in Adverse Pressure Gradient," *Journal of the Aeronautical Sciences*, Vol. 21, No. 2, 1954, pp. 91–108.

[3] Cousteix, J., and Pailhas, G., "Three-Dimensional Wake of a Swept Wing," *Proceedings of the International Symposium on Structure of Complex Turbulent Shear Flow*, edited by R. Dimas and L. Fulachier, Springer-Verlag, Berlin, 1983, pp. 376–387.

[4] Cousteix, J., Pailhas, G., and Aupoix, B., "Three-Dimensional Wake of a Swept Wing," *Proceedings 2nd Symposium on Numerical and Physical Aspects of Aerodynamic Flows*, edited by T. Cebeci, California State Univ., Long Beach, CA, Jan. 1983.

[5] Pot, P. J., "Measurement in Two-Dimensional Wake and in a Two-Dimensional Wake Merging into a Boundary Layer," National Lucht- en Ruimtevaartloboratorium, Data Rept. NLR TR 79063L, The Netherlands, 1979.

[6] Andreopoulos, J., and Bradshaw, P., "Measurements of Interacting Turbulent Shear Layers in the Near Wake of a Flat Plate," *Journal of Fluid Mechanics*, Vol. 100, No. 3, 1980, pp. 639–668.

[7] Savill, A. M., and Zhou, M. D., "Wake/Boundary Layer and Wake/Wake Interactions: Smoke Flow Visualisation and Modelling," *Proceedings 2nd Asian Congress of Fluid Mechanics*, Science Press, Beijing, 1983, pp. 743–752.

[8]Bario, F., Charnay, G., and Papailiou, K. D., "An Experiment Concerning the Confluence of a Wake and a Boundary Layer," *Journal of Fluids Engineering*, Vol. 104, No. 1, 1982, pp. 18–24.

[9]Agoropoulos, D., and Squire, L. C., "Interactions Between Turbulent Wakes and Boundary Layers," *AIAA Journal*, Vol. 26, No. 10, 1988, pp. 1194–1200.

[10]Zhou, M. D., and Squire, L. C., "The Interaction of a Wake with a Boundary Layer," *Proceedings of the International Symposium on Structure of Complex Turbulent Shear Flow*, edited by R. Dumas and L. Fulachier, Springer-Verlag, Berlin, 1983, pp. 376–387.

[11]Zhou, M. D., and Squire, L. C., "The Interaction of a Wake with a Turbulent Boundary Layer," *Aeronautical Journal*, Vol. 89, No. 882, 1985, pp. 72–81.

[12]Foster, D. N., Irwin, H. P., and Williams, B. R., "The Two-Dimensional Flow Around a Slotted Flap," Aeronautical Research Council, R and M 3681, London, 1970.

[13]Van den Berg, B., and Oskam, B., "Boundary Layer Measurements on a Two-Dimensional Wing with a Flap and a Comparison with Calculations," CP 271, AGARD, 1980.

[14]Brune, G. W., and Sikavi, D. A., "Experimental Investigation of the Confluent Boundary Layer of a Multielement Low Speed Aerofoil," AIAA Paper 83-0566, Jan. 1983.

[15]Bloy, A. W., and Trochalidis, V., "The Aerodynamic Interference Between Tanker and Receiver Aircraft During Air-to-Air Refuelling," *Aeronautical Journal*, Vol. 94, No. 935, 1990, pp. 165–171.

[16]Iversen, J. D., and Bernstein, S., "Trailing Vortex Effects on Following Aircraft," *Journal of Aircraft*, Vol. 11, No. 1, 1974, pp. 60–61.

[17]Tabachnikov, V. G., "The Study of the Hysteresis of Distributed Aerodynamic Characteristics of Large Aspect Ratio Wings," *Trudy TsAGI*, No. 2420, 1989, pp. 3–19 (in Russian).

[18]Stolyarov, G. I., and Tabachnikov, V. G., "Some Features of Aerodynamics of Large Aspect Ratio Wings at Low Reynolds Numbers," *Trudy TsAGI*, No. 2290, 1985, pp. 71–83 (in Russian).

[19]Krassilschikoff, P. P., "The Effect of Tip-Shields on the Aerodynamic Characteristic of an Airfoil," *Trudy TsAGI*, Vol. 58, 1930, pp. 1–9 (in Russian).

[20]Kornilov, V. I., and Kharitonov, A. M., "Some Features of the Near-Wall Flow in the Region of Wing/Body Junction," *Uchenye Zapiski TsAGI*, Vol. 18, No. 4, 1987, pp. 1–9 (in Russian).

[21]Kornilov, V. I., and Kharitonov, A. M., "Investigation of the Structure of Turbulent Flows in Streamwise Asymmetric Corner Configurations," *Experiments in Fluids*, Vol. 2, 1984, pp. 205–212.

[22]Marumo, E., Suzuki, K., and Sato, T., "A Turbulent Boundary Layer Disturbed by a Cylinder," *Journal of Fluid Mechanics*, Vol. 87, No. 1, 1978, pp. 121–141.

[23]Wygnanski, I., Champagne, F., and Marasli, B., "On the Large-Scale Structures in Two-Dimensional, Small-Deficit, Turbulent Wakes," *Journal of Fluid Mechanics*, Vol. 168, 1986, pp. 31–71.

[24]Novak, C. J., and Ramaprian, B. R., "Measurements in the Wake of an Infinite Swept Airfoil," Iowa Inst. of Hydraulic Research, IIHR Rept. 240, NASA Grants NSG-1200 and NAG 2-110, April 1982.

[25]So, R. M. C., and Mellor, G. L., "Experiment on Convex Curvature Effects in Turbulent Boundary Layers," *Journal of Fluid Mechanics*, Vol. 60, Pt. 1, 1973, pp. 43–62.

[26]Meroney, R. N., and Bradshaw, P., "Turbulent Boundary-Layer Growth over a Longitudinally Curved Surface," *AIAA Journal*, Vol. 13, No. 11, 1975, pp. 1448–1453.

[27]Pavlov, L. S., "An Incompressible Flow Around the Central Sections of a Swept Rectangular Wing," *Trudy TsAGI*, No. 1617, 1974 (in Russian).

[28]Sundaram, S., Viswanath, P. R., and Rudrakumar, S., "Viscous Drag Reduction Using Riblets on NACA 0012 Airfoil to Moderate Incidence," *AIAA Journal*, Vol. 34, No. 4, 1996, pp. 676–682.

[29]Boiko, A. V., Dovgal, A. V., Zanin, B. Yu., and Kozlov, V. V., "Three-Dimensional Structure of Separated Flows on Wings (Review)," *Thermophysics and Aeromechanics*, Vol. 3, No. 1, 1996, pp. 1–13.

[30]Dyban, E. P., and Epik, E. Ya., *Heat Transfer and Hydrodynamics in Turbulized Flow*, Nauk. Dumka, Kiev, Ukraine, 1985 (in Russian).

G. M. Faeth
Editor-in-Chief